A single-component, cross-linked, and surface-grafted polyelectrolyte film fabricated by the layer-by-layer assembly method

Jiang, Tao; Moghaddam, Saeed Zajforoushan; Thormann, Esben

Published in:
Polymer

Link to article, DOI:
10.1016/j.polymer.2020.122524

Publication date:
2020

Document Version
Peer reviewed version

A Single-component, Cross-linked, and Surface-grafted Polyelectrolyte Film Fabricated by the Layer-by-layer Assembly Method

Tao Jiang, Saeed Zajforoushan Moghaddam, Esben Thormann*

Department of Chemistry, Technical University of Denmark, 2800 Kgs. Lyngby, Denmark

Abstract

In this work, we demonstrate a versatile approach for the fabrication of a single-component polyelectrolyte layer with tunable thickness and functionality. Poly(ethylene glycol) methyl ether methacrylate (PEGMEMA) was copolymerized with either aminoethyl methacrylate (AMA) or methacrylic acid (MAA) to prepare statistical PEGMEMA copolymers carrying positive or negative charges, respectively. These polyelectrolytes were used in a conventional layer-by-layer assembly process followed by cross-linking to form a surface-grafted stable poly(PEGMEMA) layer carrying both negative and positive charges. To transform this layer into a single-component polyelectrolyte layer carrying just one type of ionizable group, the amino groups were quenched, thus leaving a single-component anionic PEGMEMA-based polyelectrolyte layer. Last, we demonstrate that compared to a zwitterionic layer, the anionic polyelectrolyte layer exhibits an enhanced protein-repelling property against bovine serum albumin (BSA).

Keywords: Single-component polyelectrolyte film, layer-by-layer, PEGMEMA, QCM-D, pH-responsiveness

1. Introduction

Polyelectrolyte films are thin molecular layers that consist of polymer chains with ionizable groups. The chemical composition and ionizable groups of the polyelectrolyte chains control the functional properties of the film, such as controlled permeability,[1] anti-icing,[2] and antifouling.[3] Polyelectrolyte films can be fabricated through different methods. For instance, desired polyelectrolytes have been chemically grafted onto a target substrate via either the "graft-onto" approach[4,5] or surface-initiated polymerization.[6,7] A more convenient and adaptable method is through physical adsorption of the polyelectrolyte chains onto the substrate, e.g., electrostatic adsorption onto charged surfaces.[8,9] However, the formed layer is typically only a few nanometers thick, showing modest surface coverage.[10,11]

Layer-by-layer assembly (LbL) is an alternative method for the fabrication of relatively thick polyelectrolyte films.[12–16] Herein, a polyelectrolyte multilayered (PEM) film is prepared by the sequential adsorption of oppositely charged polyelectrolytes onto a charged surface. The desired thickness of the PEM films is then realized using the number of depositions, and it can reach up to several microns.[17] Moreover, LbL assembly is a straightforward and versatile method that allows coating surfaces of different sizes and geometries. While conventional PEM films consist of at least two different polyelectrolyte components, only a handful of studies have reported the preparation of single-component multilayer films.[18–21] For instance, Liu et al. prepared a single-component chitosan film by fabricating a cross-linked chitosan/polyacrylic acid PEM and then removing the polyanion by overnight treatment with an alkaline solution.[22,23] Despite the simplicity of this approach, it lacks versatility, and incomplete removal of the second component is expected. As another approach, Tong et al. fabricated a poly(allylamine hydrochloride) (PAH) multilayer film in which glutaraldehyde-mediated covalent interactions promote the LbL assembly.[24] The fast Schiff base chemistry provides a feasible approach for repeated PAH deposition, driving film thickness growth.

Nevertheless, this method is driven by chemical bond formation and hence suffers a low layer buildup efficiency, and a high pH value is required to minimize the electrostatic repulsion between the amino groups.

Another effective method to fabricate single-component polyelectrolyte multilayered films is based on the copolymerization of a functional monomer with a charged monomer.[25] We previously copolymerized poly(ethylene glycol) methyl ether methacrylate (PEGMEMA) with 2-aminoethyl methacrylate (AMA). It was shown that the obtained PEGMEMA-based copolymer contains positive charges that are randomly distributed along the copolymer chain; hence, it can be paired with a given polyanion using the LbL assembly method.[26] Following this same approach, it is feasible to copolymerize PEGMEMA with a negatively charged monomer to prepare an anionic PEGMEMA-based copolymer. The two oppositely charged PEGMEMA-based copolymers can be paired using the LbL assembly method, yielding a polyelectrolyte film with a tunable thickness that consists of only one functional monomer.

Adopting this approach, in this work, we have fabricated a single-component PPEGMEMA multilayered film. To do so, we copolymerized PEGMEMA with AMA and methacrylic acid (MAA) to prepare positively and negatively charged PEGMEMA copolymers, respectively. The two charged PEGMEMA copolymers were LbL assembled onto a pre-aminated silica substrate to provide a PPEGMEMA multilayered film, followed by chemical cross-linking with carbodiimide chemistry to enhance the film stability and graft the film onto the substrate. Furthermore, to obtain a truly single-component PPEGMEMA polyelectrolyte film with only negative charges, the residual amino groups in the film were quenched with a PEG-terminated carboxylic acid, m-PEG3-COOH. Finally, we examined the adsorption of bovine serum albumin (BSA) on the PPEGMEMA films.

2. Experimental Section

2.1 Materials

PEGMEMA (number average molecular weight (M_n) of 300 g.mol^{-1}) and t-butyl methacrylate (99%) were purchased from Sigma-Aldrich Denmark and treated using neutral alumina column chromatography to remove the inhibitors before use. (2-Boc-Amino)ethyl methacrylate (t-BocAMA, 99%), diethyl meso-2,5-dibromoadipate (98%), trifluoroacetic acid (TFA, 99%), (3-aminopropyl)triethoxysilane (APTES, 99%) and copper(I) chloride (CuCl, >99%, washed sequentially with acetic acid and ethanol before use) were purchased from Sigma-Aldrich and used as received unless otherwise stated. Tris(2-dimethylaminoethyl)amine (Me_6TREN, 99%) was purchased from Alfa Aesar. m-PEG3-COOH (99%) was purchased from BroadPharm and used as received. All the solvents used in this work were of HPLC grade and purchased from Sigma-Aldrich. A pH 7 phosphate buffer solution (pH adjusted to 7 with 50 mM sodium hydrogen phosphate dibasic) was used for the preparation of the polymer solutions as well as in the rinsing step between each layer deposition. Solutions containing 300 ppm (w/v) P(PEGMEMA-*stat*-MAA) and P(PEGMEMA-*stat*-AMA) were prepared for LbL assembly and filtered through 0.22 μm nylon syringe filters to remove possible aggregates and dust. Ultrapure water (Sartorius Arium® Pro ultrapure water system, resistivity of 18.2 MΩ cm) was used to prepare all the solutions.

2.2 Synthesis of P(PEGMEMA-*stat*-AMA) and P(PEGMEMA-*stat*-MAA)

A two-step protocol was employed to avoid the interference of the pendant amino groups to the polymerization, as formerly reported.[27] First, PEGMEMA was copolymerized with protected t-BocAMA, yielding a P(PEGMEMA-*stat*-tBocAMA) statistical copolymer, where all the AMA units were protected by t-Boc groups. In the second step, the t-Boc groups were removed under acidic conditions (TFA/DCM), giving the desired P(PEGMEMA-*stat*-AMA)

copolymer. Briefly, for the synthesis of P(PEGMEMA-*stat*-tBocAMA), diethyl meso-2,5-dibromoadipate (7.2 mg, 0.02 mmol), PEGMEMA (M_n = 300) (900 mg, 3 mmol), t-BocAMA(229.27 mg, 1 mmol) and Me6TREN (9.2 mg, 0.04 mmol) were dissolved in 5 ml of isopropanol. Dimethylformamide (0.1 ml) was added to the reaction mixture as an internal standard for later calculation of the monomer conversion and molecular weight (M_n). The reaction mixture was purged with nitrogen gas for at least 30 min, after which prewashed copper(I) chloride (1.23 mg, 0.0125 mmol) was added. The polymerization was triggered by immersing the reaction flask in a 50 °C water bath. After 16 h, the reaction was quenched by adding 5 ml of water into the solution and exposure to air. A 0.1 ml sample of the solution was collected for proton nuclear magnetic resonance (^{1}H NMR) spectroscopy measurement to determine the reaction conversion. The polymer solution was then purified via dialysis (using regenerative cellulose tubing with an MWCO of 6-8 kDa, Spectrum Laboratories, Inc.) against water for 3 days. Finally, the residual water was removed via lyophilization to obtain the pure P(PEGMEMA-*stat*-tBocAMA) polymer. In the deprotection process, the obtained P(PEGMEMA-*stat*-tBocAMA) (300 mg) was dissolved in 4 ml of dichloromethane, followed by the addition of 0.5 ml of trifluoroacetic acid. The reaction mixture was stirred at room temperature for 3 h, after which the dichloromethane was removed by evaporation. The viscous polymer residue was redissolved in 5 ml of water, and the pH was adjusted to be approximately neutral with a 1 M NaOH solution. The polymer was purified by dialysis and subsequent lyophilization, yielding a light yellow viscous liquid. The ^{1}H NMR spectra of P(PEGMEMA-*stat*-tBocAMA) and P(PEGMEMA-*stat*-AMA) are available in our previous work.[26]

The P(PEGMEMA-*stat*-MAA) copolymer was synthesized in a similar manner. Instead of (2-Boc-amino)ethyl methacrylate, t-butyl methacrylate was added and copolymerized with PEGMEMA at the same stoichiometric ratio. All the reaction procedures, purification techniques, and characterization methods were the same as those used for P(PEGMEMA-*stat*-

AMA). The ^{1}H NMR spectra of P(PEGMEMA-*stat*-tBuMAA) and P(PEGMEMA-*stat*-MAA) are shown in Figure S1. The t-butyl protection group peak (1.4 ppm) vanished after treating with TFA, confirming successful deprotection. For nomenclature convenience, hereafter, we name P(PEGMEMA-*stat*-MAA) and P(PEGMEMA-*stat*-AMA) as PPEGMEMA- and PPEGMEMA+, respectively.

The ^{1}H NMR (Bruker 400 MHz) spectra were used to calculate the conversion and number average molecular weight (M_n). To do so, 0.1 ml samples of the reaction mixture were collected before and after the polymerization process. The ^{1}H NMR spectra of both samples were taken using deuterated dimethyl sulfoxide (DMSO) as the solvent. The integral ratios of δ 6.0 ppm (monomer double bond (vinyl)) to δ 7.9 ppm (DMF) before (r_1) and after (r_2) polymerization were calculated to compute the monomer conversion (c) via the simple relation $c = 1 - r_2/r_1$. M_n was then calculated using:

$$M_{theo} = M_i + M_{mon}c$$

where M_i and M_{mon} are the molecular weights of the initiator and the monomer, respectively.

To independently determine the number average molecular weight (M_n), weight average molecular weight (M_w), and polydispersity index (PDI) of the copolymers, asymmetric flow field-flow fractionation (AF4) was performed using a Wyatt Eclipse instrument with UV (Agilent 1230 infinity, Agilent), refractive index (Optilab rex, 633 nm, Wyatt) and multiangle light scattering (MALS) (Dawn Heleos-II, 662 nm, Wyatt) detectors. A frit-inlet channel equipped with a regenerated cellulose membrane (MWCO 5 kDa, Millipore) and a 350 µm width spacer were used as the separation channel. Each sample was analyzed with a constant detector flow of 0.5 mL/min, and a cross-flow that decreased exponentially from 3 mL min^{-1} to 0 in 20 min. A 50 mM PBS pH 7.4 buffer solution was prepared and filtered with a 0.1 µm membrane (Millipore) for use as the eluent. The samples were dissolved in the PBS buffer to

a concentration of 5 mg/ml, and the injection volume was set as 100 µL. A refractive index increment (dn/dc) value of 0.12 was determined and used in the calculation of the molecular weight and polydispersity, as described in our previous work.[26] The Astra software (Wyatt, version 7.1.3.15) was used for data analysis and calculation of the molecular weight with the Debye plot using the Zimm formula.[28] The chromatogram of PPEGMEMA+ is shown elsewhere,[26] while that of PPEGMEMA- is provided in the Supporting Information (Figure S2).

2.3 Quartz crystal microbalance with dissipation monitoring (QCM-D)

2.3.1 Instrumentation and theory

The LbL assembly and pH-responsiveness of the PPEGMEMA+/PPEGMEMA- multilayer films were monitored with QCM-D (Q-Sense E1, Biolin Scientific, Gothenburg, Sweden) using silica-coated sensors (QSX 303, Biolin Scientific). In a typical QCM-D experiment, a quartz crystal sensor undergoes an oscillating voltage, leading to the corresponding oscillation at its resonance frequency (F). In addition, the sensor oscillation amplitude is monitored throughout the decay, and the dissipation factor (D) is calculated as the dissipated energy divided by the total stored energy. For thin, uniform and rigid films, the frequency shifts are proportional to the adsorbed mass per unit area, which is modeled by the Sauerbrey equation. However, the Sauerbrey equation provides a valid estimation only if the ratio of dissipation and normalized frequency shifts is sufficiently small (i.e., if $(\Delta D_n)/(-\Delta f_n/n)$ is smaller than 4×10^{-7} Hz^{-1}) so that the film can simplistically regarded as rigid.[29] In contrast, for soft and highly hydrated polymeric films, the so-called effective coupled mass depends on how the oscillatory acoustic wave propagates through the attached film. Consequently, the coupled water (either bound or unbound) and the viscous drag force will additionally contribute to the frequency shifts. Under this condition, the viscoelastic Voigt model provides a better

estimation of the adsorbed mass, where the adhered film is represented by a layer of uniform thickness and density with distinct viscous and elastic components. Accordingly, the frequency and dissipation shifts are related to the properties of the film and the medium following [30]:

$$\frac{\Delta f}{f} = -\frac{d_f \rho_f}{d_q \rho_q}\left(1 - \eta_0 \rho_0 \times \frac{(\eta_f/\rho_f)\omega^2}{\left(\mu_f^2 + \omega^2 \eta_f^2\right)}\right)$$

$$\Delta D = \frac{d_f}{d_q \rho_q}\left(\eta_0 \rho_0 \times \frac{\mu_f \omega}{\mu_f^2 + \omega^2 \eta_f^2}\right)$$

where ω is the angular frequency of the oscillation, η_0 and ρ_0 are the viscosity and density of the medium, respectively, and d_q and ρ_q are the thickness and density of the quartz crystal resonator, respectively. To avoid overparameterization, the medium density, medium viscosity, and film density are estimated and then treated as fixed parameters in the model. Therefore, the thickness (d_f), viscosity (η_f) and shear modulus (μ_f) of the polymeric film are obtained by fitting the Voigt model to the measured shifts in frequency and dissipation for different overtones (3rd, 5th and 7th). The instrument software (QSense® Dfind, v1.1, Biolin Scientific) was employed for modeling the data. The density of the film (ρ_f) was estimated to be 1040 $kg \cdot m^{-3}$. The density and viscosity of water at 23 °C (provided in the software library) were used for the medium.

2.3.2 LbL assembly

The sensor underwent a pre-amination process with APTES before the LbL assembly.[31] To do so, the sensor was rinsed with copious amounts of ethanol and water, dried, and then plasma-cleaned (PDC-32G plasma cleaner, Harrick Plasma) in water vapor with a constant pressure of 0.5 Torr for 1 min. The clean sensor was placed in an evacuated desiccator with a 50% (v/v) APTES/toluene solution for 18 h to allow for the deposition of APTES onto the surface. Thereafter, the sensor was rinsed with copious amounts of toluene and ethanol and dried with compressed air. The sensor was then immediately mounted in the QCM-D module, and the

measurement was started at 23 °C using a 75 μL/min flow of phosphate buffer (pH 7). Upon achieving a stable baseline for all the harmonics, PPEGMEMA+ and PPEGMEMA- solutions were alternately loaded (30 min for each layer) and rinsed (20 min for each layer) with buffer to obtain 7 bilayers in total. To cross-link the fabricated film, a 10 mg/mL EDC/NHS solution was flowed over the sensor for 12 h, after which the chamber was rinsed with pH 7 buffer to remove the residual EDC/NHS. To further quench the amino groups and remove the positive charges on the film, an m-PEG3-COOH solution (10 mg/ml m-PEG3-COOH, 10 mg/ml EDC/NHS) was flowed over the sensor for 12 h. To test the pH stability, NaCl solutions at pH 2.5, 7 and 10 (100 mM, pH-adjusted with HCl/NaOH) were loaded to perform 3 consecutive pH cycles.

2.3.3 Test of BSA repellence

To test the antifouling property of the film, the adsorption of BSA on the films was investigated. First, a baseline was obtained using a pH 7.4 phosphate buffer, after which a 5% w/w BSA solution (50 mg/mL) was flowed over the sensor for 20 min. Subsequently, the chamber was rinsed with pH 7.4 phosphate buffer to remove unbound BSA. The adsorbed mass of BSA was estimated via the Sauerbrey relation[32], $\Delta m = -\frac{C\Delta f}{n}$, where Δm is the absorbed BSA mass, Δf is the frequency shift, n is the overtone number (1, 3, 5,…,13), and C (17.7 ng/cm^2) is the mass-sensitivity constant for the 5 M Hz quartz crystal. The frequency shift of the third overtone was used for the mass calculation.

3. Results and discussion

3.1 Synthesis of PPEGMEMA+ and PPEGMEMA-

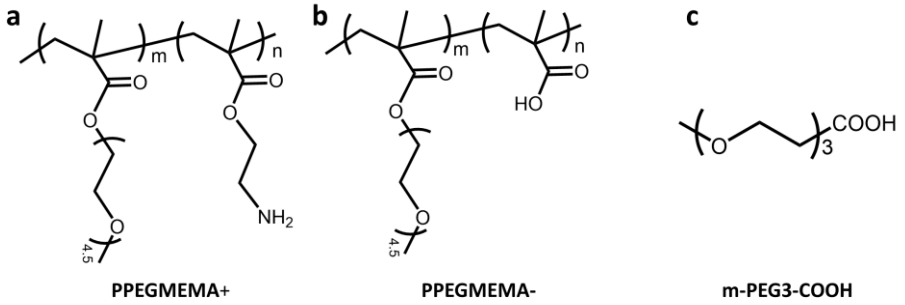

Figure 1 (a) Structure of cationic PPEGMEMA+; (b) structure of anionic PPEGMEMA-; and (c) structure of the mPEG3-COOH used to quench the amino groups in the multilayered films.

PEGMEMA-based polycation (PPEGMEMA+) and polyanion (PPEGMEMA-) were synthesized with a statistical copolymerization process by ATRP, in which primary amino groups and carboxyl groups are distributed randomly along the copolymer chains, respectively. The chemical structures of the synthesized copolymers are presented in Figure 1 and a summary of their characteristics are given in Table 1. The amount of acidic or basic groups on each of the two polymers is 25%. The molecular weights of the two copolymers were measured with AF4, and the M_n values of the two polymers exhibit an overall good agreement with those obtained from ^{1}H NMR spectroscopy. The PDI values of the two polymers are approximately 1.7, which is relatively high for ATRP polymerization. However, this high value is not a concern with respect to the LbL assembly process.

Table 1 Properties of the synthesized charge-bearing PPEGMEMA copolymers

	Polymer Composition							
	PEGMEMA	AMA	MAA	Mn[a] (kDa)	Mn[b] (kDa)	PDI[b]	Amine content (DP%)	Methacrylic acid content (DP%)
PPEGMEMA+	135	45	-	46.7	38.3	1.71	25%	-
PPEGMEMA-	99	-	33	32.5	29.0	1.74	-	25%

a. Determined with ^{1}H NMR spectroscopy; b. Determined with AF4

3.2 LbL assembly of PPEGMEMA+/PPEGMEMA-

The LbL assembly of PPEGMEMA+ and PPEGMEMA- was monitored in situ with QCM-D. The shifts in the resonance frequency (F) and dissipation factor (D) resulting from multilayer deposition are presented in Figure 2. The resonance frequency relates to the total (effective) mass coupled with the sensor, including the deposited polymer chains and the associated water content. The dissipation factor is, on the other hand, a semiquantitative measure of the layer conformation; i.e., a higher dissipation factor corresponds to a more viscoelastic layer. The odd and even layer numbers refer to the deposition of the PPEGMEMA- and PPEGMEMA+ layers, respectively. Overall, 7 bilayers of the PEGMEMA copolymers were deposited on the silica sensor. Following the deposition steps, general trends of an increase in the dissipation factor and decrease in the resonance frequency are observed, together indicating consistent polymer mass deposition on the surface. The largest frequency and dissipation shifts are observed for the first deposited bilayer, which can be attributed to the high positive charge density of the APTES-functionalized silica surface. However, after the first couple of bilayer depositions, the QCM-D shifts show a rather linear dependence on the number of layers indicating a stable growth of the PPEGMEMA multilayered film. The overall frequency shift for the 7 bilayers is approximately -70 Hz, and the dissipation shift value is approximately 9.5, yielding a $\Delta D/(-\Delta f)$ value of approximately 0.14×10^{-6}. This ratio indicates a rather viscoelastic behavior that can be attributed to the hydrated nature of the film due to the abundant presence of the PEG units.[33,34] This observation is further in accordance with our previous study,[26] where relatively large dissipation shifts were observed.

The viscoelastic Voigt model was fitted to the frequency and dissipation shifts to estimate the acoustic thickness of the prepared PEM film. The overall thickness of the 7-bilayer PEM film is approximately 17 nm at the conditions where the layer is fabricated (phosphate buffer at pH 7). In a similar manner, the acoustic thickness demonstrates a rather linear dependence on the

layer number after the first deposited bilayer. The first deposited bilayer shows an estimated thickness of approximately 6 nm, followed by a steady thickness growth of approximately 1.5 nm per bilayer.

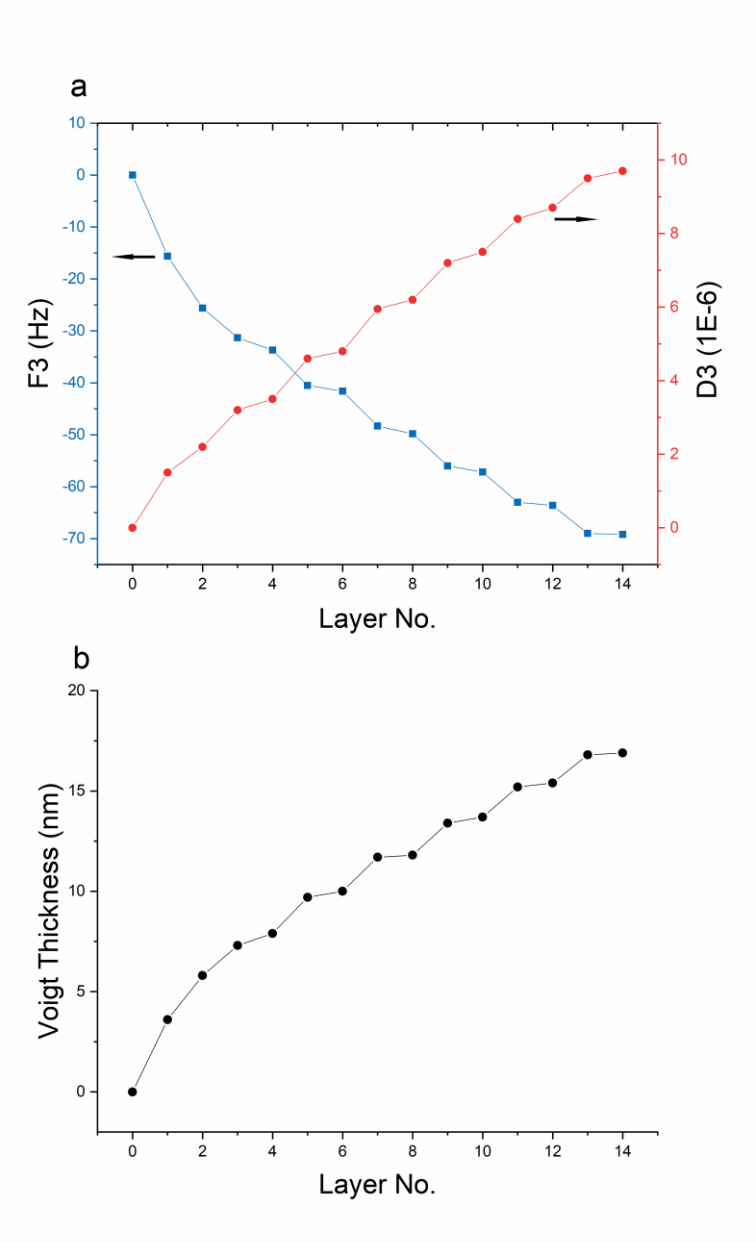

Figure 2 QCM-D monitoring of LbL of PPEGMEMA+/PPEGMEMA- in pH 7 phosphate buffer; (a) frequency and dissipation shifts; (b) film thicknesses obtained by Voigt modeling

3.3 Cross-linking the PPEGMEMA+/PPEGMEMA- films

Weak polyelectrolyte multilayer films are subject to disintegration (dissolution) in response to pH variations due to the consequent charge imbalance in the film.[35–37] Figure 3a shows the QCM-D data corresponding to the pH stability test on the prepared PPEGMEMA+/PPEGMEMA- multilayered film. Accordingly, when the pH is switched from 7 to 2.5, a drastic increase in the frequency and decrease in the dissipation are found. In addition, the frequency and dissipation shifts are completely irreversible, since the initial values of frequency and dissipation are not restored when the pH is returned to 7. Repeated pH cycling confirms the irreversible mass loss and disintegration of the PPEGMEMA+/PPEGMEMA- film, indicating the instability of the PEM film due to the positive charge imbalance produced when the pH is changed from 7 to 2.5.

To enhance the stability of the PEM film, the multilayered film can be chemically cross-linked using EDC/NHS amidation chemistry. EDC/NHS is a highly efficient cross-linker that catalyzes the amide formation reaction between the carboxyl and amino groups in the film. In addition, amidation between the APTES-treated substrate and the first PPEGMEMA- layer is expected to graft the entire film onto the substrate. Hence, a surface-grafted and cross-linked PEM with enhanced stability should be obtained. The film stability towards pH variations was examined again after the film was exposed to a 10 mg/ml EDC/NHS solution for 12 h prior to any change in pH after the LbL assembly process (Figure 3b). When the pH is decreased from 7 to 2.5, an increase in the dissipation and decrease in the frequency were observed, indicating a swelling behavior of the film. This result is in accordance with previous reports regarding the pH-responsive behavior of cross-linked weak polyelectrolyte multilayers.[23,26,35] When the pH is returned from 2.5 to 7, a decrease in the dissipation and an increase in the frequency are found, which together indicate the shrinkage of the film back to its initial state. This pH cycling was repeated three times, and despite a minor hysteresis, a reversible and repeatable swelling-

shrinking process is observed, indicating a significantly more stable and surface-grafted PEM film, as well as a pH-responsiveness of the cross-linked multilayered film.

To test the stability of the film under alkaline conditions, the pH was repeatedly cycled between 7 and 10. Accordingly, increasing the pH from 7 to 10 results in an increase in the dissipation and a decrease in the frequency, indicating a swelling behavior of the film. Decreasing the pH back to 7 gives rise to a decrease in the frequency and an increase in the dissipation, suggesting shrinkage of the multilayered film. It is noteworthy that the QCM-D shifts when the pH is changed from 10 to 7 are larger than those when the pH is increased from 7 to 10, which might be due to a loss of unbound PPEGMEMA polymer chains and/or a structural reorganization of the film. Nevertheless, after the first pH cycle, the film exhibits only minor hysteresis and repeatable swelling-shrinking behavior when the pH is shifted between 7 and 10, implying a high film stability under alkaline conditions.

The observed dual pH-responsiveness of the film indicates the presence of unreacted amine and carboxyl groups in the film. At pH 7, where the LbL assembly is conducted, the film is found in a charge-neutral state where the number of charged amino groups and carboxyl groups within the film are comparable. At this “zwitterionic” state, the film adopts a collapsed conformation. By decreasing the pH from 7 to 2.5, the amine and carboxyl groups undergo a protonation process, leading to a net positive charge imbalance in the film. The film thus exhibits an overall cationic state, and hence, a swollen conformation is found due to the osmotic pressure difference, as discussed in our previous work.[26] When the pH is increased from 7 to 10, the deprotonation of amine and carboxyl groups leads to a net negative charge imbalance within the film. Consequently, the film exhibits an overall anionic state and adopts a swollen conformation.

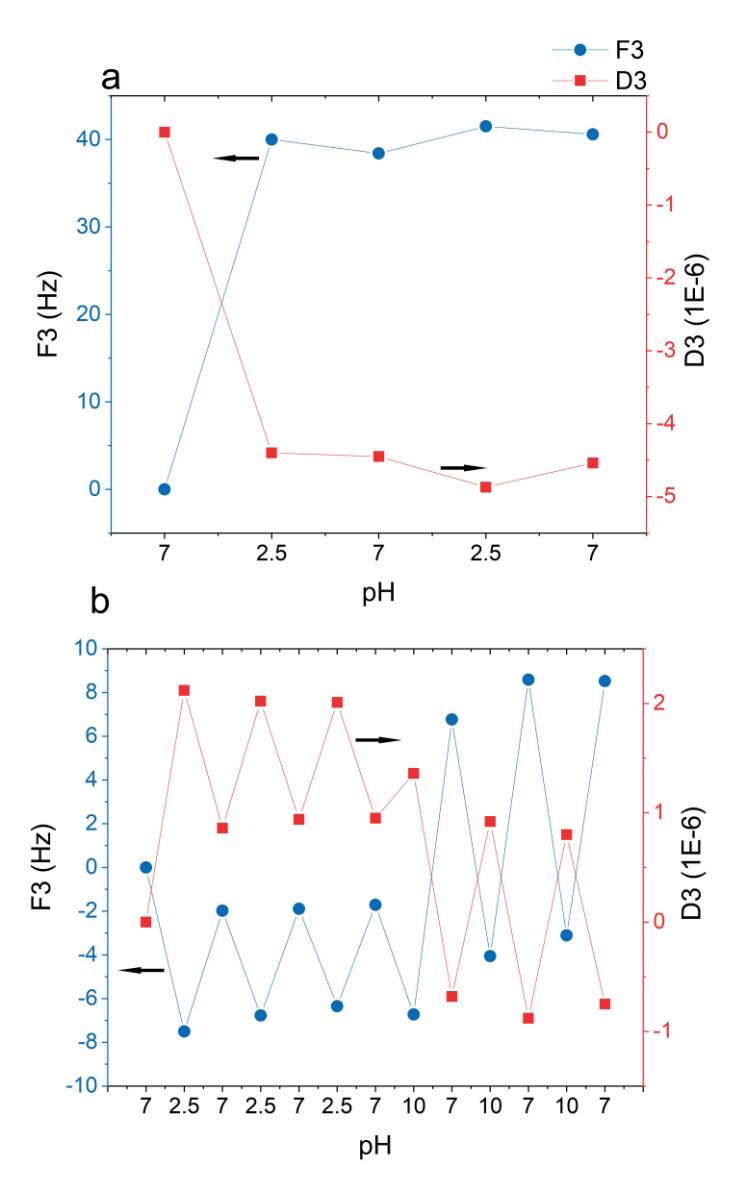

Figure 3 Frequency (blue circle) and dissipation (red square) shifts of PPEGMEMA+/PPEGMEMA- film during repeated pH cycles from 2.5 to 7 for (a) a non-cross-linked system and (b) a system cross-linked with EDC/NHS for 12 h

3.4 Transformation from PPEGMEMA+/PPEGMEMA- to a single-component PPEGMEMA- polyelectrolyte film

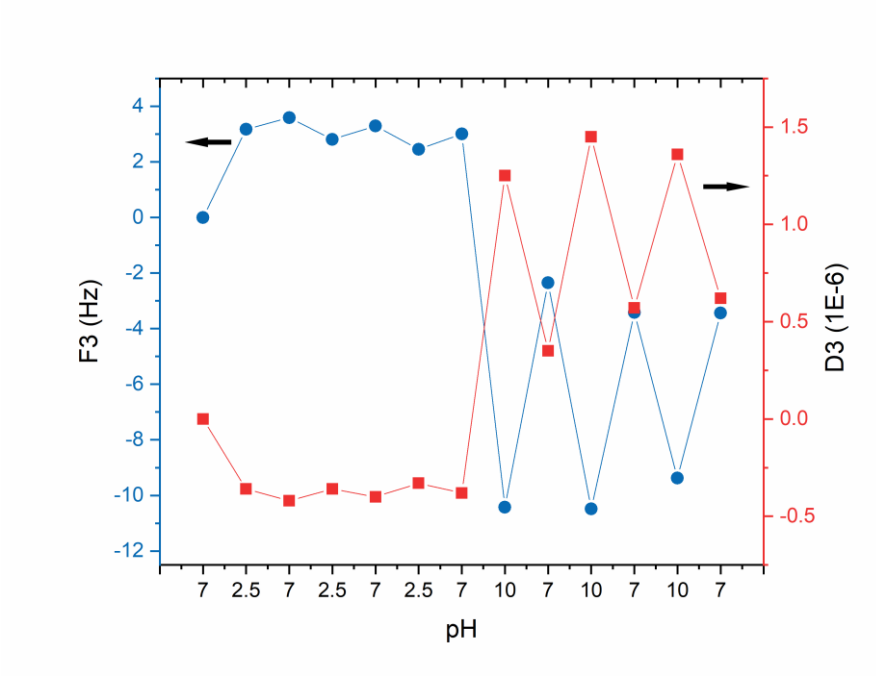

Figure 4 Frequency (blue circle) and dissipation (red square) shifts of PPEGMEMA- polyelectrolyte film as a function of pH during pH cycles from 2.5 to 7 after amine quenching with m-PEG3-COOH

As described in Figure 3, the stabilized (cross-linked) PPEGMEMA+/PPEGMEMA- multilayer film contains both amine and carboxyl groups, and it will thus demonstrate a zwitterionic state under neutral pH conditions. To obtain a genuine single-component polyelectrolyte film similar to a layer consisting of just one type of copolymer (PPEGMEMA-), the excess amino groups in the film are quenched via the same EDC/NHS chemistry utilized in the cross-linking process. To do so, a PEGylated carboxylic acid (m-PEG3-COOH) was dissolved into the EDC/NHS solution and was loaded into the QCM chamber for 12 h. Consequently, the amino groups were replaced by short PEG units via amide formation.

Figure 4 displays the QCM-D data of the pH cycles performed on the film after the amine quenching process. By decreasing the pH from 7 to 2.5, an increase in the frequency and a decrease in the dissipation were observed, probably due to the removal of the unbound cross-

linking agent and a reorganization of the film. Nevertheless, further cycling of the pH between 7 and 2.5 results in negligible shifts of the frequency (~1 Hz) and dissipation (< 0.1). The loss of pH-responsiveness and the swelling of the film under acidic conditions confirm the successful quenching of the amino groups within the film. In contrast, the film shows pH-responsiveness and swelling under alkaline conditions, a behavior similar to that observed before the amine quenching process. Therefore, by means of amine quenching, the zwitterionic film is converted into a single-component, negatively charged PPEGMEMA polyelectrolyte film.

3.5 Investigation of BSA repellence

To demonstrate the functional differences between the single-component PEM and the two-component PEM (carrying both negative and positive charges), we finally studied the adsorption of BSA to the single-component and two-component films. PEG and its derivatives have been extensively investigated as promising materials for protein-resistant coatings.[38–40] Since proteins contain charged groups, the electrostatic state of a coating can contribute to the protein-coating interactions.[41] At a neutral pH, BSA carries a net negative charge, and by choosing BSA we therefore can investigate the potentially higher protein repellence of the anionic single-component PEM compared to the zwitterionic two-component PEM. To do so, a 5% (w/w %) BSA solution in pH 7.4 phosphate buffer was loaded into the QCM-D cell for 20 min, followed by 20 min of rinsing with the phosphate buffer. Figure 5 illustrates the frequency shifts resulting from the adsorption of BSA on bare silica, the two-component zwitterionic film (before amine quenching), and the negatively charged single-component film (after amine quenching). As a reference substrate, the adsorption of BSA is first assessed on a bare silica sensor, which indicates a frequency decrease of approximately 32 Hz, corresponding to an adsorbed mass of approximately 570 ng/cm^2. For the two-component PPEGMEMA film (before amine quenching), a frequency decrease of approximately 11 Hz is found, which

corresponds to an adsorbed mass of approximately 190 ng/cm^2. Finally, for the negatively charged single-component PPEGMEMA film (after amine quenching), a frequency shift of approximately -5 Hz is observed, corresponding to an adsorbed BSA mass of 90 ng/cm^2. Accordingly, the multilayered films, in general, reduce BSA adsorption compared to that on bare silica. However, it is also shown that the positive charges in the zwitterionic PEM have a negative impact on the BSA repellence, and the removal of the amino group leads to a further reduction in BSA adsorption. To this end it should be noted that the positively charged amino group were neutralized by the incorporation of short PEG units from m-PEG3-COOH, which might add to the BSA repellant properties of the single-component PPEGMEMA film.

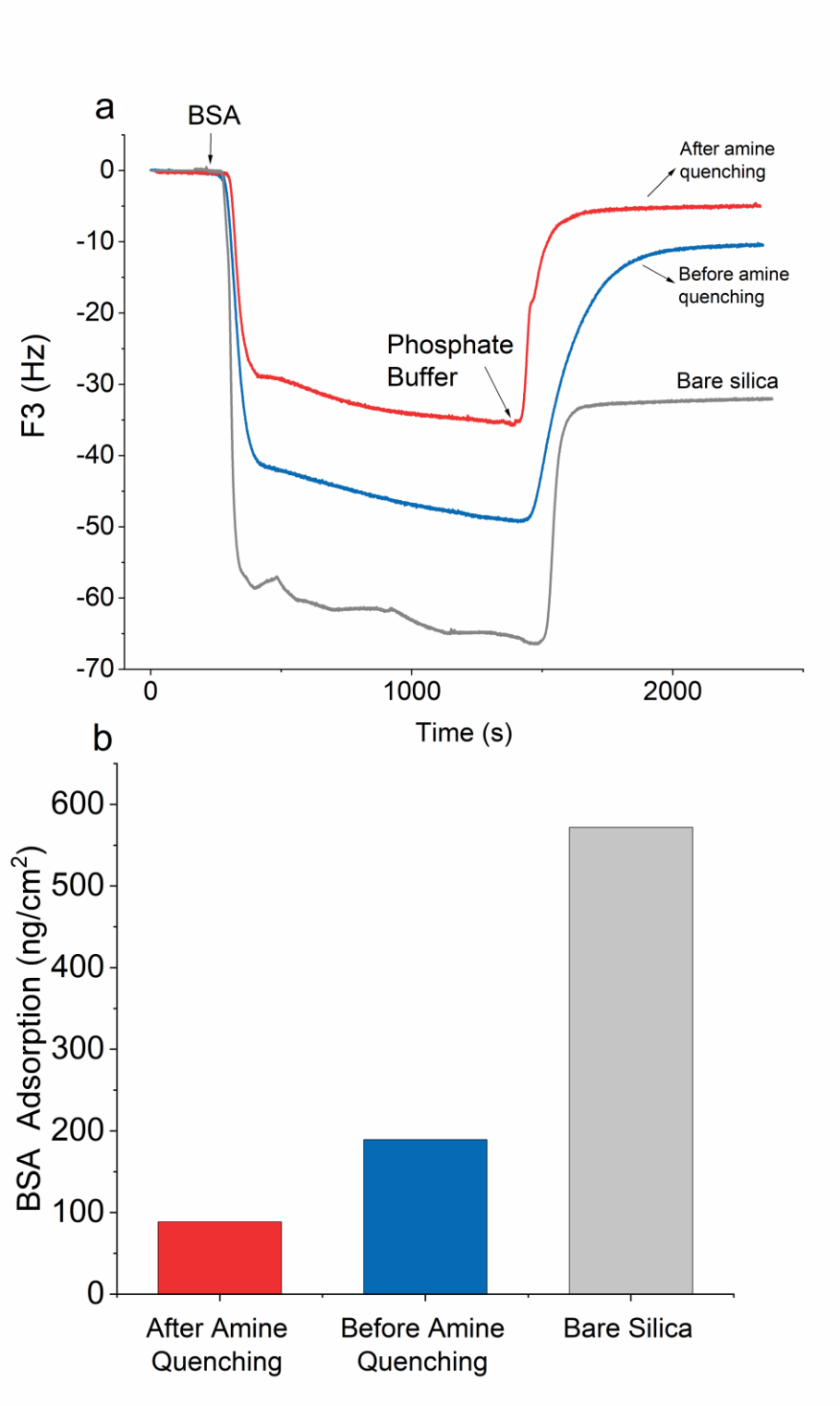

Figure 5 Surface fouling test with 5% (w/w %) BSA adsorption: (a) frequency shifts obtained from QCM-D and (b) BSA mass absorbed calculated accordingly for bare silica (gray), the cross-linked PPEGMEMA coating before amine quenching (blue) and after amine quenching with m-PEG3-COOH (red)

4. Conclusion

In this work, we proposed a versatile approach to prepare a surface-grafted single-component polyelectrolyte film with a tunable film thickness. Two oppositely charged PEGMEMA copolymers were first synthesized and then LbL assembled. In situ monitoring of the LbL assembly by QCM-D demonstrated successful layer buildup, with an approximately 17 nm film obtained in 7 bilayers. The multilayered film was then cross-linked using EDC/NHS chemistry to chemically graft onto the aminated substrate and enhance the film stability towards pH variations. The cross-linked film exhibited swelling under both acidic and basic conditions without experiencing disintegration of the film or significant mass loss. To obtain a truly single-component PPEGMEMA polyelectrolyte film, the amino groups in the film were quenched with m-PEG3-COOH, leaving behind only the negatively charged carboxyl groups. After the quenching process, the film shows no swelling under acidic conditions, while its pH-responsiveness under alkaline conditions is retained, indicating successful elimination of the amino groups. The single-component PPEGMEMA polyelectrolyte film also demonstrated a relatively high resistance against BSA adsorption. In conclusion, the proposed method might serve as a convenient and efficient approach to fabricate a functional single-component polyelectrolyte film with tunable thickness by using the LbL assembly approach.

Acknowledgement

We would like to acknowledge the financial support from the Independent Research Fund Denmark (grant # 6111-00102B).

*Corresponding author contact: esth@kemi.dtu.dk, +45 4525-2439

References

[1] J. Wu, M.J. Sailor, Chitosan hydrogel-capped porous SiO2 as a pH responsive nano-valve for triggered release of insulin, Adv. Funct. Mater. 19 (2009) 733–741. https://doi.org/10.1002/adfm.200800921.

[2] S. Chernyy, M. Järn, K. Shimizu, A. Swerin, S.U. Pedersen, K. Daasbjerg, L. Makkonen, P. Claesson, J. Iruthayaraj, Superhydrophilic polyelectrolyte brush layers with imparted anti-icing properties: Effect of counter ions, ACS Appl. Mater. Interfaces. 6 (2014) 6487–6496. https://doi.org/10.1021/am500046d.

[3] G. Cheng, Z. Zhang, S. Chen, J.D. Bryers, S. Jiang, Inhibition of bacterial adhesion and biofilm formation on zwitterionic surfaces, Biomaterials. 28 (2007) 4192–4199. https://doi.org/10.1016/j.biomaterials.2007.05.041.

[4] P.G. Hartley, S.L. McArthur, K.M. McLean, H.J. Griesser, Physicochemical Properties of Polysaccharide Coatings Based on Grafted Multilayer Assemblies, Langmuir. 18 (2002) 2483–2494. https://doi.org/10.1021/la001801i.

[5] M. Benz, N. Chen, J. Israelachvili, Lubrication and wear properties of grafted polyelectrolytes, hyaluronan and hylan, measured in the surface forces apparatus, J. Biomed. Mater. Res. 71A (2004) 6–15. https://doi.org/10.1002/jbm.a.30123.

[6] M. Ballauff, O. Borisov, Polyelectrolyte brushes, Curr. Opin. Colloid Interface Sci. 11 (2006) 316–323. https://doi.org/10.1016/j.cocis.2006.12.002.

[7] J.O. Zoppe, N.C. Ataman, P. Mocny, J. Wang, J. Moraes, H.A. Klok, Surface-Initiated Controlled Radical Polymerization: State-of-the-Art, Opportunities, and Challenges in Surface and Interface Engineering with Polymer Brushes, Chem. Rev. 117 (2017) 1105–1318. https://doi.org/10.1021/acs.chemrev.6b00314.

[8] T. Pettersson, A. Naderi, R. Makuška, P.M. Claesson, Lubrication properties of bottle-brush polyelectrolytes: An AFM study on the effect of side chain and charge density, Langmuir. 24 (2008) 3336–3347. https://doi.org/10.1021/la703229n.

[9] S.A. Sukhishvili, S. Granick, Polyelectrolyte adsorption onto an initially-bare solid surface of opposite electrical charge, J. Chem. Phys. 109 (1998) 6861–6868. https://doi.org/10.1063/1.477253.

[10] N.G. Hoogeveen, M.A. Cohen Stuart, G.J. Fleer, Polyelectrolyte adsorption on oxides. I. Kinetics and adsorbed amounts, J. Colloid Interface Sci. 182 (1996) 133–145. https://doi.org/10.1006/jcis.1996.0444.

[11] T. Saarinen, M. Österberg, J. Laine, Properties of cationic polyelectrolyte layers adsorbed on silica and cellulose surfaces studied by QCM-D-effect of polyelectrolyte charge density and molecular weight, J. Dispers. Sci. Technol. 30 (2009) 969–979. https://doi.org/10.1080/01932690802646488.

[12] J. Borges, J.F. Mano, Molecular Interactions Driving the Layer-by-Layer Assembly of Multilayers, Chem. Rev. 114 (2014) 8883–8942. https://doi.org/10.1021/cr400531v.

[13] J.J. Richardson, M. Bjornmalm, F. Caruso, Technology-driven layer-by-layer assembly of nanofilms, Science. 348 (2015) aaa2491–aaa2491. https://doi.org/10.1126/science.aaa2491.

[14] G. Decher, Fuzzy Nanoassemblies: Toward Layered Polymeric Multicomposites, Science. 277 (1997) 1232–1237. https://doi.org/10.1126/science.277.5330.1232.

[15] X. Zhu, X. Jun Loh, Layer-by-layer assemblies for antibacterial applications, Biomater. Sci. 3 (2015) 1505–1518. https://doi.org/10.1039/C5BM00307E.

[16] S. Zhao, F. Caruso, L. Dähne, G. Decher, B.G. De Geest, J. Fan, N. Feliu, Y. Gogotsi, P.T. Hammond, M.C. Hersam, A. Khademhosseini, N. Kotov, S. Leporatti, Y. Li, F. Lisdat, L.M. Liz-Marzán, S. Moya, P. Mulvaney, A.L. Rogach, S. Roy, D.G. Shchukin, A.G. Skirtach, M.M. Stevens, G.B. Sukhorukov, P.S. Weiss, Z. Yue, D. Zhu, W.J. Parak, The Future of Layer-by-Layer Assembly: A Tribute to ACS Nano Associate Editor Helmuth Möhwald, ACS Nano. 13 (2019) 6151–6169. https://doi.org/10.1021/acsnano.9b03326.

[17] C. Porcel, P. Lavalle, V. Ball, G. Decher, B. Senger, J.C. Voegel, P. Schaaf, From Exponential to Linear Growth in Polyelectrolyte Multilayers, Langmuir. 22 (2006) 4376–4383. https://doi.org/10.1021/la053218d.

[18] Y. Zhang, Y. Guan, S. Zhou, Single component chitosan hydrogel microcapsule from a layer-by-layer approach, Biomacromolecules. (2005). https://doi.org/10.1021/bm050058b.

[19] Y. Wang, V. Bansal, A.N. Zelikin, F. Caruso, Templated Synthesis of Single-Component Polymer Capsules and Their Application in Drug Delivery, Nano Lett. 8 (2008) 1741–1745. https://doi.org/10.1021/nl080877c.

[20] U. Manna, J. Dhar, R. Nayak, S. Patil, Multilayer single-component thin films and microcapsules via covalent bonded layer-by-layer self-assembly, Chem. Commun. 46 (2010) 2250. https://doi.org/10.1039/b924240f.

[21] X. Liang, V. Kozlovskaya, Y. Chen, O. Zavgorodnya, E. Kharlampieva, Thermosensitive Multilayer Hydrogels of Poly(N -vinylcaprolactam) as Nanothin Films and Shaped Capsules, Chem. Mater. 24 (2012) 3707–3719. https://doi.org/10.1021/cm301657q.

[22] C. Liu, E. Thormann, P.M. Claesson, E. Tyrode, Surface Grafted Chitosan Gels. Part I. Molecular Insight into the Formation of Chitosan and Poly(acrylic acid) Multilayers, Langmuir. 30 (2014) 8866–8877. https://doi.org/10.1021/la5013186.

[23] C. Liu, E. Thormann, P.M. Claesson, E. Tyrode, Surface Grafted Chitosan Gels. Part II. Gel Formation and Characterization, Langmuir. 30 (2014) 8878–8888. https://doi.org/10.1021/la501319r.

[24] T. Weijun, G. Changyou, H. Möhwald, Single polyelectrolyte microcapsules fabricated by glutaraldehyde-mediated covalent layer-by-layer assembly, Macromol. Rapid Commun. 27 (2006) 2078–2083. https://doi.org/10.1002/marc.200600533.

[25] J.A. Jaber, J.B. Schlenoff, Polyelectrolyte multilayers with reversible thermal responsivity, Macromolecules. 38 (2005) 1300–1306. https://doi.org/10.1021/ma0485235.

[26] T. Jiang, S. Zajforoushan Moghaddam, E. Thormann, PPEGMEMA-based cationic copolymers designed for layer-by-layer assembly, RSC Adv. 9 (2019) 26915–26926. https://doi.org/10.1039/C9RA05464B.

[27] M.-H. Dufresne, J.-C. Leroux, Study of the Micellization Behavior of Different Order

Amino Block Copolymers with Heparin, Pharm. Res. 21 (2004) 160–169. https://doi.org/10.1023/B:PHAM.0000012164.60867.c6.

[28] B.H. Zimm, The Scattering of Light and the Radial Distribution Function of High Polymer Solutions, J. Chem. Phys. 16 (1948) 1093–1099. https://doi.org/10.1063/1.1746738.

[29] I. Reviakine, D. Johannsmann, R.P. Richter, Hearing what you cannot see and visualizing what you hear: Interpreting quartz crystal microbalance data from solvated interfaces, Anal. Chem. 83 (2011) 8838–8848. https://doi.org/10.1021/ac201778h.

[30] M. V. Voinova, M. Rodahl, M. Jonson, B. Kasemo, Viscoelastic Acoustic Response of Layered Polymer Films at Fluid-Solid Interfaces: Continuum Mechanics Approach, Phys. Scr. 59 (1999) 391–396. https://doi.org/10.1238/Physica.Regular.059a00391.

[31] F. Zhang, K. Sautter, A.M. Larsen, D.A. Findley, R.C. Davis, H. Samha, M.R. Linford, Chemical vapor deposition of three aminosilanes on silicon dioxide: Surface characterization, stability, effects of silane concentration, and cyanine dye adsorption, Langmuir. 26 (2010) 14648–14654. https://doi.org/10.1021/la102447y.

[32] G. Sauerbrey, Use of a quartz vibrator for weighing thin films on a microbalance, Zeitschrift Für Phys. 155 (1959) 206–222. https://doi.org/10.1007/BF01337937.

[33] J. Malmström, H. Agheli, P. Kingshott, D.S. Sutherland, Viscoelastic modeling of highly hydrated laminin layers at homogeneous and nanostructured surfaces: Quantification of protein layer properties using QCM-D and SPR, Langmuir. 23 (2007) 9760–9768. https://doi.org/10.1021/la701233y.

[34] F. Höök, B. Kasemo, T. Nylander, C. Fant, K. Sott, H. Elwing, Variations in coupled water, viscoelastic properties, and film thickness of a Mefp-1 protein film during adsorption and cross-linking: A quartz crystal microbalance with dissipation monitoring, ellipsometry, and surface plasmon resonance study, Anal. Chem. 73 (2001) 5796–5804. https://doi.org/10.1021/ac0106501.

[35] K. Glinel, C. Déjugnat, M. Prevot, B. Schöler, M. Schönhoff, R. v. Klitzing, Responsive polyelectrolyte multilayers, Colloids Surfaces A Physicochem. Eng. Asp. 303 (2007) 3–13. https://doi.org/10.1016/j.colsurfa.2007.02.052.

[36] C. Ďjugnat, G.B. Sukhorukov, pH-responsive properties of hollow polyelectrolyte microcapsules templated on various cores, Langmuir. 20 (2004) 7265–7269. https://doi.org/10.1021/la049706n.

[37] A.I. Petrov, A.A. Antipov, G.B. Sukhorukov, Base-acid equilibria in polyelectrolyte systems: From weak polyelectrolytes to interpolyelectrolyte complexes and multilayered polyelectrolyte shells, Macromolecules. 36 (2003) 10079–10086. https://doi.org/10.1021/ma034516p.

[38] V.B. Damodaran, S.N. Murthy, Bio-inspired strategies for designing antifouling biomaterials, Biomater. Res. 20 (2016) 1–11. https://doi.org/10.1186/s40824-016-0064-4.

[39] I. Banerjee, R.C. Pangule, R.S. Kane, Antifouling coatings: Recent developments in the design of surfaces that prevent fouling by proteins, bacteria, and marine organisms, Adv. Mater. 23 (2011) 690–718. https://doi.org/10.1002/adma.201001215.

[40] Q. Yu, Y. Zhang, H. Wang, J. Brash, H. Chen, Anti-fouling bioactive surfaces, Acta

Biomater. 7 (2011) 1550–1557. https://doi.org/10.1016/j.actbio.2010.12.021.

[41] D.S. Salloum, J.B. Schlenoff, Protein adsorption modalities of polyelectrolyte multilayers, Biomacromolecules. 5 (2004) 1089–1096. https://doi.org/10.1021/bm034522t.